

# Spatially-resolved high-power high-temperature Raman spectroscopy as an effective tool for probing the microscopic structural variations in complex alloys: CZTSe as an example

Qiong Chen <sup>a</sup>, Sergio Bernadi <sup>b</sup> and Yong Zhang <sup>a</sup>

<sup>a</sup>Department of Electrical and Computer Engineering, and Energy Production and Infrastructure Center (EPIC), The University of North Carolina at Charlotte, Charlotte, NC 28223, USA

<sup>b</sup>CEA, LITEN, 17 rue des Martyrs, 38054 Grenoble Cedex 9, France

**Abstract** — We show that nominally similar CZTSe films may differ significantly in their microscopic structures that cannot be easily revealed by applying conventional characterization tools, including conventional Raman. CZTSe films prepared by sputtering and co-evaporation are examined in both lateral and depth direction to demonstrate the effectiveness of this spectroscopy method.

## I. INTRODUCTION

Different fabrication techniques represent different paths to the efficiency limit set by Shockley–Queisser limit. Even two techniques yield comparable efficiencies, the absorber layers could be different in their microscopic structures. It is of great interest to know the differences. TEM is commonly viewed as the most reliable and accurate technique for structural analysis, but it is destructive and inefficient. Raman spectroscopy is an effective tool for chemical composition and structural analyses of materials. It is typically used under the assumption that the probe light intensity is sufficiently low such that no structural change has been induced by the perturbation. In this work, we use “high power (HP)” or “high excitation density” Raman spectroscopy involving a tightly focused CW laser with a power density that is just high enough to introduce a local structural change, and probe the change using “low power (LP)”. Performing spatially resolved Raman mapping on an as-grown material can already reveal composition and/or structural variations in the sample. However, the application of the HP Raman spectroscopy can reveal some subtle but important structural differences in two samples that might otherwise appear to be indistinguishable under the normal probes, such as LP Raman, PL, XRD, and device characteristic. HP Raman spectroscopy, in conjunction with the high spatial resolution of the confocal optics, is a very powerful approach for probing the structural inhomogeneity, in particular in a complex alloy like  $\text{Cu}_2\text{ZnSnSe}_4$  (CZTSe), with much greater efficiency and/or sensitivity than TEM and other laser spectroscopy techniques.

## II. EXPERIMENTAL DETAILS

All Raman measurements were performed with a Horiba Jobin Yvon HR800 confocal Raman system using a 532 nm

laser. The room temperature measurement was carried out with a 100x objective lens with NA = 0.9. The diffraction limit laser spot size is 0.76  $\mu\text{m}$ , and the spatial resolution of the measurement is about half of the laser spot size. A 50x long working distance lens with NA = 0.5, was used in high temperature Raman tests. Sample was heated by Linkam TS1500 heating system with temperature control accuracy of 1  $^\circ\text{C}$ .

Two bare CZTSe film samples were studied. CZTSe\_97 (S1) was prepared by selenizing the metal stacks which composed of 300 nm Mo, 130 nm Zn, 155 nm Cu and 180 nm Sn sputtered on an Ashai PV 200 glass substrate. The film compositions are  $[\text{Zn}]/[\text{Sn}] \cong 1.25$  and  $[\text{Cu}]/([\text{Zn}]+[\text{Sn}]) \cong 0.85$ , and the thickness is slightly higher than 1  $\mu\text{m}$ . A device with nominally similar absorber was measured with  $\sim 5\%$  efficiency. M3599\_12 (S2) was grown by a vacuum co-evaporation method on a soda lime glass substrate, with 1  $\mu\text{m}$  sputtered Mo back contact and 150  $\text{\AA}$  e-beam evaporated NaF precursor. The film thickness and composition of S2 are 1.49  $\mu\text{m}$ ,  $[\text{Zn}]/[\text{Sn}] \cong 1.32$  and  $[\text{Cu}]/([\text{Zn}]+[\text{Sn}]) \cong 0.82$ . A device with the nominally same absorber had an efficiency of  $\sim 8\%$ .

## III. RESULTS AND DISCUSSIONS

### A. Raman Studies from Front Surface

In Fig. 1 plotted in dash curves, typical LP Raman spectra from two CZTSe samples were obtained from their front surface with 0.147 mW ( $3.5 \times 10^4 \text{ W/cm}^2$ ) laser power. Both CZTSe films showed two intense Raman peaks 195 – 196  $\text{cm}^{-1}$ , 172 – 173  $\text{cm}^{-1}$ , and a weak peak at 232 – 233  $\text{cm}^{-1}$ , which are very close to the single crystal Raman scattering peaks at 196, 173 and 231  $\text{cm}^{-1}$  [1]. Additional peaks at 221.8, 222.7, 243.9 – 244.4, 249.2 and 251– 252.7  $\text{cm}^{-1}$  were also observed. Among them, the 221– 223  $\text{cm}^{-1}$  peak is believed to be a TO Raman mode from kesterite structure based on calculations [2-4]. 244– 245  $\text{cm}^{-1}$  was also reported to be CZTSe related both experimentally and theoretically [5-7]. The presence of secondary phase  $\text{Cu}_2\text{SnSe}_3$  contributes to weak peaks located near 251  $\text{cm}^{-1}$  [1]. ZnSe was observed at 252.7  $\text{cm}^{-1}$ . Amorphous selenium (a-Se) was reported to display a Raman feature at  $\sim 250 \text{ cm}^{-1}$  and a shoulder at  $\sim 235 \text{ cm}^{-1}$  when crystallized trigonal Se (t-Se)

exists in a-Se [8]. It is also possible that selenium is present in CZTSe films since they were fabricated in a Se-rich condition. The origin of the broad band ranging from 380 to 390  $\text{cm}^{-1}$  is still unclear.

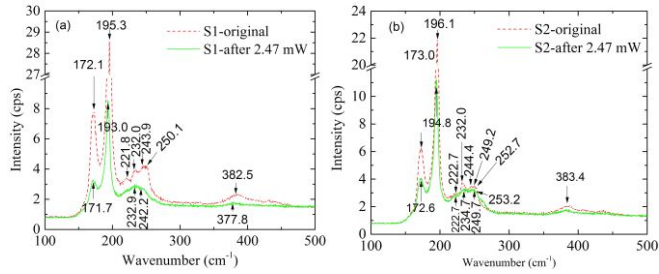


Fig. 1. Raman spectra of two CZTSe samples after tested spots being illuminated by 2.47 mW.

High laser power effect on CZTSe Raman scattering was observed by comparing Raman spectra taken at the same spot before and after HP illumination. For each sample, after taking the Raman spectrum shown in red, the same spot was illuminated with 2.47 mW ( $5.9 \times 10^5 \text{ W/cm}^2$ ) for 100 seconds, then the Raman spectrum was re-measured with 0.146 mW under the same conditions. After the HP illumination, the illuminated spot showed some color change, becoming lighter under optical microscope, but no apparent ablation. The results for the two samples are shown in Fig. 1 green curves. The two main CZTSe peak at 195 – 196  $\text{cm}^{-1}$  and 171 – 172  $\text{cm}^{-1}$  experienced not only intensity reduction, but also red shift in both samples. Besides, some new peaks appeared after HP illumination. In Fig. 1 (a), a new Raman peak at 242  $\text{cm}^{-1}$  was observed from S1. This 242  $\text{cm}^{-1}$  peak matches  $A_{1g}$  Raman mode of  $\text{MoSe}_2$  [9]. For S2 in Fig. 1 (b), new peak appeared at 234.7  $\text{cm}^{-1}$  which is close to the 235  $\text{cm}^{-1}$  shoulder from crystallized trigonal Se (t-Se) observed in a-Se [8].

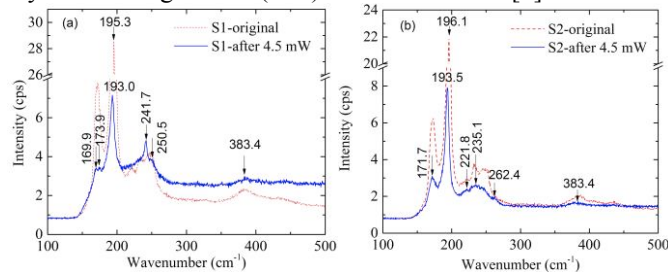


Fig. 2. Raman spectra of two CZTSe samples after tested spots being illuminated by 4.5 mW.

The laser power was further increased to 4.5 mW ( $1.1 \times 10^6 \text{ W/cm}^2$ ) to illuminate the same spot for 36 seconds. Raman data were collected again with 0.147 mW power. As shown in Fig. 3 (a), the intensity of 193  $\text{cm}^{-1}$  peak of S1 is only 10% of its original value before high power illumination, and the 172  $\text{cm}^{-1}$  mode became a weak shoulder from 168  $\text{cm}^{-1}$  to 178  $\text{cm}^{-1}$ . In addition, a sharp and strong peak appears at 241.7  $\text{cm}^{-1}$ , which is enhanced from the 242.2  $\text{cm}^{-1}$  peak in Fig. 1 (a). Interestingly, the main CZTSe peak intensity only dropped by a factor of four, and the  $\sim 172 \text{ cm}^{-1}$  CZTSe peak remains sharp in S2 after 4.5

mW illumination. Furthermore, the 242  $\text{cm}^{-1}$  peak do not appear as shown in Fig. 2(b). Obviously, HP illumination brought qualitatively different changes to the two samples. The contrast between S1 and S2 suggests that there are some subtle microscopic differences between the two samples.

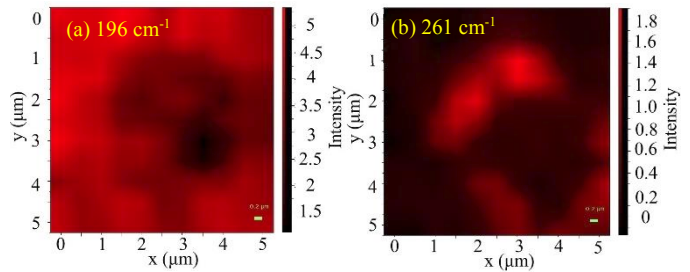


Fig. 3. S1 Raman mapping after one spot being illuminated by 2.47 mW for 100s.

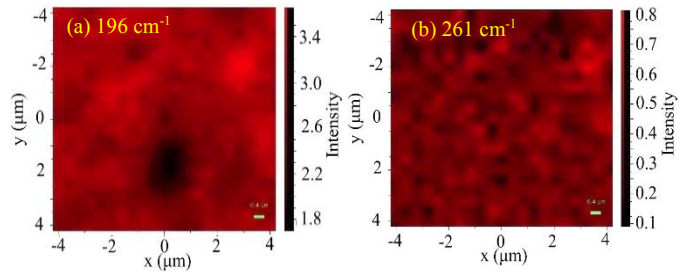


Fig. 4. S2 Raman mapping after one spot being illuminated by 2.47 mW for 100s.

2D Raman mapping was performed to examine the spatial extension of the local heating effect caused by the high power illumination on CZTSe sample surface. One random spot from each sample surface was first illuminated by 2.47 mW for 100s, Raman mapping was then acquired from a  $5 \times 5 \mu\text{m}$  (Fig. 3) or  $8 \times 8 \mu\text{m}$  (Fig. 4) square centered at the illuminated spot with 0.147 mW laser power. For S1, in addition to the CZTSe mode at 196  $\text{cm}^{-1}$ , another peak  $\sim 261 \text{ cm}^{-1}$  was also observed as a ring near the illuminated site. Figs. 3 and 4 show, respectively for the two samples, Raman intensity mapping results at 196  $\text{cm}^{-1}$  and 261  $\text{cm}^{-1}$ . Dark circles in Figs. 3 and 4(a) confirmed the intensity drop of the CZTSe main Raman modes at 196  $\text{cm}^{-1}$ . For S1, with the darkest  $\sim 1 \mu\text{m}$  circle at the illumination site, a dark circle with diameter of  $\sim 3 \mu\text{m}$  showed lower intensity at 196  $\text{cm}^{-1}$  peak, which is much larger than the laser spot size  $\sim 0.76 \mu\text{m}$ . Moreover, a ring which encloses the illuminated spot was found rich in  $\text{Cu}_x\text{Se}_y$  suggested by a strong Raman peak at 261  $\text{cm}^{-1}$ , as shown in Fig. 3 (b). For S2, on the other hand, 2.47 mW laser illumination only affected a range  $\sim 1.5 \mu\text{m}$  circle, Fig. 4(a), and did not generate a  $\text{Cu}_x\text{Se}_y$  ring, Fig. 4(b). The difference between S1 and S2 seems to suggest that the two nominally similar films might have different thermal conductivities, and also that CZTSe absorber prepared by sputtering method is more sensitive to high power illumination than film fabricated by co-evaporation method.

### (B) Raman Studies from Cleaved Edge

Raman spectra were measured from cleaved edge with laser beam focused to different depths of the sample: Mo layer, Mo-CZTSe boundary, body of film, film-air boundary and air (when the beam was just moved off the edge of the front surface). Because of the limitation of the laser spot size, these measurements can only reveal the qualitative changes. Measured at lower power condition (0.147 mW) from the cleaved edge, one can clearly see the variation of the spectral features with film depth in Fig. 5. For S1, MoSe<sub>2</sub> is dominant component at the substrate-film boundary with Raman modes at 169, 242, 286 and 351 cm<sup>-1</sup> in S1. The mode ~196 cm<sup>-1</sup> appears in both Mo and CZTSe layers, although substantially weaker in the Mo region. When moving toward the front surface, the MoSe<sub>2</sub> related peaks gradually diminish, whereas the CZTSe peaks at 196 cm<sup>-1</sup> and 172 cm<sup>-1</sup> grow. In contrast, no Raman signal from MoSe<sub>2</sub> was observed near the substrate of S2.

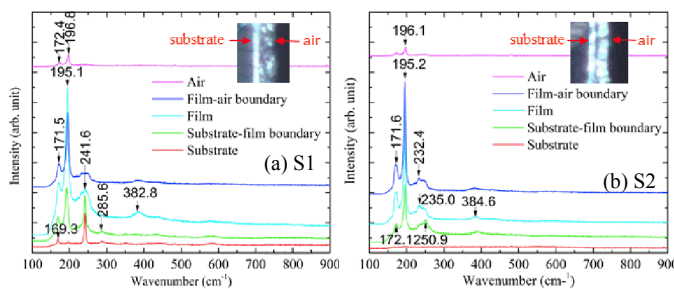


Fig. 5. Raman spectra of two CZTSe samples measured from cleaved edge.

The measured cleaved edge spots were then illuminated by 2.47 mW for 100 seconds and Raman spectra from these spots were collected again with 0.147 mW. In addition to red shift, a very weak peak at 262.3 cm<sup>-1</sup> was observed when laser moved beyond the CZTSe film. However, No new peak appeared from S2 cleaved edge after being illuminated by 2.47 mW. Increasing the illumination laser power to 4.5 mW for 36 seconds, Cu<sub>x</sub>Se<sub>y</sub> Raman mode at 261.5 cm<sup>-1</sup> could also be observed from S2 cleaved edge spectra. Besides, a peak at 263.1 cm<sup>-1</sup> which is close to Cu<sub>x</sub>Se<sub>y</sub> Raman mode showed up in the Raman spectrum from substrate of S1, as shown in Fig. 6. Additionally, many new peaks were detected at its substrate and CZTSe film boundary, such as SnSn peak 185.6 cm<sup>-1</sup>, ZnSe peak at 202.6 cm<sup>-1</sup>, and some other peaks at 729.3 cm<sup>-1</sup> and 819.0 cm<sup>-1</sup> which are very close the molybdenum oxide Raman modes. The result of cleaved edge Raman after high power laser illumination from S1 confirms this process  $2\text{Cu}_2\text{ZnSnSe}_4 + \text{Mo} \rightarrow 2\text{Cu}_2\text{Se} + 2\text{ZnSe} + 2\text{SnSe} + \text{MoSe}_2$  predicted in Ref. [10] with co-existence of MoSe<sub>2</sub>, ZnSe, SnSe and Cu<sub>x</sub>Se<sub>y</sub> near the substrate and film boundary. However, in Fig. 6(b), only secondary phases Cu<sub>2</sub>SnSe<sub>3</sub> /a-Se and Cu<sub>x</sub>Se<sub>y</sub> but no ZnSe or MoSe<sub>2</sub> was found. These observations again indicate the microscopic structure of the polycrystalline CZTSe film could vary substantially with deposition method.

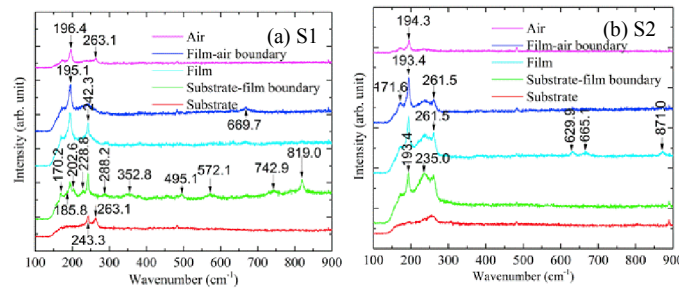


Fig. 6. Raman spectra of two CZTSe samples measured from cleaved edge after being illuminated by 4.5 mW..

#### IV. CONCLUSIONS

High power micro-Raman studies were performed on two CZTSe samples: sputtered and co-evaporated film. In general, HP illumination brought more changes to sputtered film, not only in the CZTSe Raman peaks but also in the secondary phases, which suggests that films prepared by the sputtering methods is structurally less robust than that of films fabricated by the co-evaporation method. HP Raman study is demonstrated as an effective approach to examine the microscopic structural variations of the complex alloys like CZTSe that might otherwise appear to be similar in their simple room temperature Raman spectra and device performance.

#### ACKNOWLEDGEMENT

We greatly appreciate Dr. I. Repins (NREL) for kindly providing the samples and valuable comments.

#### REFERENCE

- [1] M. Altosaar, J. Raudoja, K. Timmo, M. Danilson, M. Grossberg, J. Krustok, *et al.*, "Cu<sub>2</sub>Zn<sub>1-x</sub>Cdx Sn (Se<sub>1-y</sub>Sy) 4 solid solutions as absorber materials for solar cells," *physica status solidi (a)*, vol. 205, pp. 167-170, 2008.
- [2] A. Khare, B. Himmetoglu, M. Johnson, D. J. Norris, M. Cococcioni, and E. S. Aydil, "Calculation of the lattice dynamics and Raman spectra of copper zinc tin chalcogenides and comparison to experiments," *Journal of Applied Physics*, vol. 111, p. 083707, 2012.
- [3] M. Dimitrievska, A. Fairbrother, E. Saucedo, A. Pérez-Rodríguez, and V. Izquierdo-Roca, "Influence of compositionally induced defects on the vibrational properties of device grade Cu<sub>2</sub>ZnSnSe<sub>4</sub> absorbers for kesterite based solar cells," *Applied Physics Letters*, vol. 106, p. 073903, 2015.
- [4] T. Gürel, C. Sevik, and T. Çağm, "Characterization of vibrational and mechanical properties of quaternary compounds Cu<sub>2</sub>ZnSnS<sub>4</sub> and Cu<sub>2</sub>ZnSnSe<sub>4</sub> in kesterite and stannite structures," *Physical Review B*, vol. 84, p. 205201, 2011.
- [5] M. Grossberg, J. Krustok, K. Timmo, and M. Altosaar, "Radiative recombination in Cu<sub>2</sub>ZnSnSe<sub>4</sub> monograins studied by photoluminescence spectroscopy," *Thin Solid Films*, vol. 517, pp. 2489-2492, 2009.
- [6] M. Grossberg, J. Krustok, J. Raudoja, K. Timmo, M. Altosaar, and T. Raadik, "Photoluminescence and Raman study of Cu<sub>2</sub>ZnSn (Se<sub>x</sub>S<sub>1-x</sub>)<sub>4</sub> monograins for photovoltaic applications," *Thin Solid Films*, vol. 519, pp. 7403-7406, 2011.

- [7] A. Redinger, K. Hönes, X. Fontané, V. Izquierdo-Roca, E. Saucedo, N. Valle, *et al.*, "Detection of a ZnSe secondary phase in coevaporated  $\text{Cu}_2\text{ZnSnSe}_4$  thin films," *Applied Physics Letters*, vol. 98, p. 101907, 2011.
- [8] V. V. Poborchii, A. V. Kolobov, and K. Tanaka, "An in situ Raman study of polarization-dependent photocrystallization in amorphous selenium films," *Applied physics letters*, vol. 72, p. 1167, 1998.
- [9] T. Sekine, M. Izumi, T. Nakashizu, K. Uchinokura, and E. Matsuura, "Raman scattering and infrared reflectance in 2H-MoSe<sub>2</sub>," *Journal of the Physical Society of Japan*, vol. 49, pp. 1069-1077, 1980.
- [10] J. J. Scragg, P. J. Dale, D. Colombara, and L. M. Peter, "Thermodynamic Aspects of the Synthesis of Thin-Film Materials for Solar Cells," *ChemPhysChem*, vol. 13, pp. 3035-3046, 2012.